First-Principles Calculations on Stabilization of Iron Carbides (Fe_3C, Fe_5C_2, and η-Fe_2C) in Steels by Common Alloying Elements

CHAITANYA KRISHNA ANDE and MARCEL H.F. SLUITER

The control of carbide formation is crucial for the development of advanced low-alloy steels. Hence, it is of great practical use to know the (de)stabilization of carbides by commonly used alloying elements. Here, we use *ab initio* density functional theory (DFT) calculations to calculate the stabilization offered by common alloying elements (Al, Si, P, S, Ti, V, Cr, Mn, Ni, Co, Cu, Nb, Mo, and W) to carbides relevant to low-alloy steels, namely cementite (Fe_3C), Hägg (Fe_5C_2), and eta-carbide (η-Fe_2C). All alloying elements are considered on the Fe sites of the carbides, whereas Al, Si, P, and S are also considered on the C sites. To consider the effect of larger supercell size on the results of (de)stabilization, we use both $1 \times 1 \times 1$ and $2 \times 2 \times 2$ supercells in the case of Fe_3C.

DOI: 10.1007/s11661-012-1229-y

I. INTRODUCTION

IN advanced low-alloy steels, it is important to retain austenite to ambient temperature, and in this regard, C acts as an efficient austenite stabilizer. The precipitation of carbides in steel depletes the amount of C available for austenite stabilization, hence, it is desirable to suppress the formation of most carbide phases in advanced steels. The most commonly observed carbides in low-alloy steels are cementite (Fe_3C), Hägg carbide (Fe_5C_2), and eta-carbide (η-Fe_2C). The easiest way to suppress carbide phases is by adding alloying elements that destabilize them. Therefore, it is of interest to know quantitatively to what degree various alloying elements affect carbide stability. Although experimentally it might be difficult to control and observe the occurrence of very small precipitates of the three carbide structures in steels, it will be shown that it is rather straightforward to compute the main enthalpic contribution of alloying elements to carbide stability by first-principles methods.

Experimentally, it was found that η-Fe_2C forms first in quenched steels at temperatures between 370 K (100 °C) and 470 K (200 °C).[1,2] But, it was also noticed that ϵ-Fe_2C is the only carbide forming up to 520 K (250 °C) and forms along with cementite till 600 K (330 °C) and that it acts as a precursor for the formation of Fe_5C_2.[3,4] A long aging study at 300 K (30 °C) followed by a brief 405 K (130 °C) anneal showed the presence of both η-Fe_2C and ϵ-Fe_2C.[5] ϵ-Fe_2C is a nonstoichiometric carbon deficient structure of η-Fe_2C. It was recently shown that ϵ-Fe_2C is only slightly more unstable than η-Fe_2C and that it can relax to the latter structure.[6] Above 720 K (450 °C), it has been observed that Fe_3C forms exclusively.[1,2] Roughly, the carbides seem to precipitate in the order η-Fe_2C, Fe_5C_2, and Fe_3C with increasing temperature[6,7] with the appearance of ϵ-Fe_2C preceding η-Fe_2C. Both kinetic and thermodynamic factors could be responsible for this observation. But the predominance of each of the carbide in a definite temperature range has been attributed to the lowering of its free energy (and hence stabilization) with temperature.[6] The precipitation sequence can be altered by the application of a magnetic field thereby showing that the magnetic free energy plays an important role in the stabilization of the carbide phases.[6,8,9]

Several *ab initio* studies on pure and impurity substituted cementite have been already performed. Electronic, structural, and magnetic properties of pure cementite were described in many previous communications.[7,10–12] Furthermore, there are detailed studies of thermodynamic properties of pure cementite,[9,13] elastic properties,[14–17] point defects, and possible C diffusion paths.[12] The energetics and electronic structure of impurity substituted cementite have also been the focus of a considerable number of previous studies.[11,18–30] The partitioning behavior of alloying elements between cementite and ferrite has been described,[31] and the stabilization of cementite by various alloying elements has been studied.[20–30] In most previous computational work on the stabilization of carbide phases by alloying elements, conclusions were based on enthalpies of formation with respect to the pure carbide phase. Recently, the authors of this article argued that carbide stabilization must be evaluated based on partitioning enthalpies instead of formation enthalpies.[31]

CHAITANYA KRISHNA ANDE, formerly Doctoral Researcher, Materials innovation institute (M2i), Mekelweg 2, 2628 CD, Delft, the Netherlands, is now Postdoctoral Researcher, Plasma and Materials Processing Group, Department of Applied Physics, Eindhoven University of Technology, P.O. Box 513, 5600 MB, Eindhoven, the Netherlands. MARCEL H.F. SLUITER, Associate Professor, is with the Department of Materials Science and Engineering, Delft University of Technology, 3mE, Mekelweg 2, 2628 CD, Delft, the Netherlands. Contact email: M.H.F.Sluiter@tudelft.nl
Manuscript submitted May 5, 2011.
Dedicated to the memory of our colleague and friend Jeroen Colijn of Tata Steel, IJmuiden, the Netherlands.
Article published online June 9, 2012

Relatively less attention has been paid to the carbides Fe_5C_2 and Fe_2C, for both pure and impurity substituted phases. The electronic, magnetic, and structural properties of Fe_3C, Fe_5C_2, and η-Fe_2C have been reported.[7] Formation enthalpies,[7,33] surface properties,[34] thermodynamic properties, and formation enthalpies[6] of Fe_5C_2 have also been described. Comparable work, excluding the surface properties, has been done on η-Fe_2C.[6,7,15] Calculations have been interpreted to show that whereas Mn and Al stabilize ϵ-Fe_2C, Si destabilizes it.[27] To the best of our knowledge, no work has been done on the stabilization of either η-Fe_2C or Fe_5C_2 by alloying elements.

In this article, adding to our previous work on alloying-element-substituted FeC_3,[31] we calculate the stabilization of Fe_5C_2 and η-Fe_2C by various alloying elements. Therefore, we can now comment on relative stabilization and address the question whether alloying species (dis)favor one carbide in relation to another. Moreover, although we have not considered substitution of the alloying elements on the C site in our previous communication,[31] in this article we consider Al, Si, P, and S on the C site of the carbides. To investigate supercell effects on stabilization, we consider two supercells, $1 \times 1 \times 1$ and $2 \times 2 \times 2$, in the case of impurity-substituted cementite. We first describe the crystal structures of the carbides, then elucidate the calculation methodology of carbide (de)stabilization, and finally, we describe our results on the role of alloying elements on (de)stabilization of the carbides with respect to ferrite and the competition between carbides.

II. METHODOLOGY

Representing $Fe_{km}C_{kn}$ as the pure carbide supercell, where k is the number of formula units used to model the pure Fe_mC_n carbide, and $Fe_{km-1}MC_{kn}$ as the alloying-element-substituted carbide supercell, the balance for the formation of alloying-element-substituted carbide from the elements is given as

$$(km-1)\mathrm{Fe} + \mathrm{M} + kn\mathrm{C} \rightleftharpoons \mathrm{Fe}_{km-1}\mathrm{MC}_{kn} \qquad [1]$$

The formation enthalpy of the impurity substituted carbide is given as

$$H_f[\mathrm{Fe}_{km-1}\mathrm{MC}_{kn}] = H[\mathrm{Fe}_{km-1}\mathrm{MC}_{kn}] - (km-1)H[\mathrm{Fe}] - H[\mathrm{M}] - knH[\mathrm{C}] \qquad [2]$$

where $H[\mathrm{Fe}_{km-1}\mathrm{MC}_{kn}]$ is the enthalpy of the alloying-element-substituted cementite. $H[\mathrm{Fe}], H[\mathrm{M}]$, and $H[\mathrm{C}]$ are the enthalpies of the elements (used as reference phases) at their respective room temperature and pressure crystal structures. A similar balance and formation enthalpy applies to the pure carbide $Fe_{km}C_{kn}$ and the C site substituted carbide $Fe_{km}C_{kn-1}M$.

The stabilization of a carbide by an alloying element is usually given[20,27] by the change in formation enthalpy of the alloying-element-substituted carbide with respect to the pure carbide as

$$\Delta H_f[\mathrm{Fe}_{km-1}\mathrm{MC}_{kn}] = H_f[\mathrm{Fe}_{km-1}\mathrm{MC}_{kn}] - H_f[\mathrm{Fe}_{km}\mathrm{C}_{kn}] \qquad [3]$$

or, in terms of compound enthalpies as,

$$\Delta H_f[\mathrm{Fe}_{km-1}\mathrm{MC}_{kn}] = H[\mathrm{Fe}] + H[\mathrm{Fe}_{km-1}\mathrm{MC}_{kn}] - H[\mathrm{M}] - H[\mathrm{Fe}_{km}\mathrm{C}_{kn}] \qquad [4]$$

Similar equations apply for the C site substituted carbide.

To overcome the shortcoming of using the alloying element in its ambient temperature and pressure crystal structure as the reference state, we use another quantity defined as the partitioning enthalpy.[31] The partitioning enthalpy looks at stabilization of the carbide phase by the alloying element as a competition for the alloying element between the carbide phase and the ferrite phase. In the carbide phase, the alloying element can either occupy the Fe site or the C site. Depending on which site the alloying element occupies, we have two balances that determine the partitioning enthalpy. To compute the partitioning enthalpy for Fe substitution, the balance is given as

$$\mathrm{Fe}_{p-1}\mathrm{M} + \mathrm{Fe}_{km}\mathrm{C}_{kn} \rightleftharpoons \mathrm{Fe}_p + \mathrm{Fe}_{km-1}\mathrm{MC}_{kn} \qquad [5]$$

The partitioning enthalpy for Fe substitution is given as

$$H_p^{(\mathrm{Fe})} = H[\mathrm{Fe}_p] + H[\mathrm{Fe}_{km-1}\mathrm{MC}_{kn}] - H[\mathrm{Fe}_{p-1}\mathrm{M}] - H[\mathrm{Fe}_{km}\mathrm{C}_{kn}]) \qquad [6]$$

where $\mathrm{Fe}_p, \mathrm{Fe}_{p-1}\mathrm{M}, H[\mathrm{Fe}_p]$, and $H[\mathrm{Fe}_{p-1}\mathrm{M}]$ represent pure body-centered cubic(bcc-)Fe, the dilute solid solution of M in bcc-Fe, and their enthalpies, respectively.

Similar equations for C substitution are given as

$$\mathrm{Fe}_{p-1}\mathrm{M} + \frac{nk-1}{nk}\mathrm{Fe}_{km}\mathrm{C}_{kn} \rightleftharpoons \frac{np-(n+m)}{np}\mathrm{Fe}_p + \mathrm{Fe}_{km}\mathrm{C}_{kn-1}\mathrm{M} \qquad [7]$$

$$H_p^{(C)} = \frac{np-(n+m)}{np}H[\mathrm{Fe}_p] + H[\mathrm{Fe}_{km}\mathrm{C}_{kn-1}\mathrm{M}] - H[\mathrm{Fe}_{p-1}\mathrm{M}] - \frac{nk-1}{nk}H[\mathrm{Fe}_{km}\mathrm{C}_{kn}] \qquad [8]$$

A negative value for the partitioning enthalpy implies a stabilization of the carbide, whereas a positive value indicates stabilization of bcc-Fe. The partitioning enthalpy has been recognized as the main driving force for partitioning elsewhere also, *e.g.*, in Eqs. [11] and [14] in the work by Benedek *et al.*[35] We will show in this article, that the stabilization of an alloying element substituted carbide with respect to ferrite can be wrongly predicted when using ΔH_f instead of H_p. For the first-principles calculations, we consider the (alloying-element-substituted) carbides and (alloying-element-substituted) bcc-Fe in their 0 K ferromagnetic (FM) state.

A. *Computational Details*

We used the spin-polarized generalized gradient approximation to density functional theory (DFT)[36,37]

and a plane wave basis with a kinetic energy cut-off of 400 eV. The Kohn-Sham equations were solved using the Vienna *ab initio* simulation package (VASP, version 4.6.36 Computational Materials Physics, Vienna, Austria).[38–40] The valence electron and core interactions were described using the projector augmented wave method.[41] The first-order Methfessel-Paxton method was used with a smearing width of 0.1 eV. The PW91 exchange correlation functional[42] with the Vosko–Wilk–Nusair interpolation[43] for the correlation part was used. Structural relaxations were considered converged when the energy in two consecutive ionic relaxation steps differed by less than 10 μeV and the maximum force (worst case) on any atom in the supercell was less than 40 meV/Å. Both volume and ionic positions were relaxed in all supercells considered. For accurate bulk energies, a final calculation was done without any relaxation using the linear tetrahedron method including the Blöchl corrections.[44] Integrations in reciprocal-space employed evenly spaced Monkhorst-Pack sampling[45] such that the product of the number of k-points in the first Brillouin zone and the number of atoms in the supercell equaled approximately 10,000. Both the k-point density and energy cutoff were verified to give total energy convergence of 1 meV/supercell or better. Pure elements, except Fe, were modeled using the unit cells (or primitive cells when possible) of their respective crystal structures. Co and Ni were considered FM, and Cr was considered antiferromagnetic. It is well known that current DFT exchange-correlation functionals do not model graphite accurately. To overcome this shortcoming, the enthalpy of diamond was computed and a correction of −17 meV was added to account for the diamond to graphite transformation.[46] Pure bcc-Fe was modeled with a 128-atom supercell Fe_{128} consisting of $4 \times 4 \times 4$ bcc-Fe unit cells. We used a $3 \times 3 \times 3$ bcc-Fe supercell with 54 atoms in our previous work.[31] The $1 \times 1 \times 1$ Fe_3C supercell is the same as its unit cell with 16 atoms, it is modeled as $Fe_{12}C_4$, whereas its $2 \times 2 \times 2$ supercell with eight unit cells was modeled as $Fe_{96}C_{32}$. Fe_5C_2 was modeled using its unit cell with 28 atoms, $Fe_{20}C_8$. η-Fe_2C was modeled with $2 \times 2 \times 3$ unit cells with 72 atoms, $Fe_{48}C_{24}$. Alloying-atom-substituted supercells were modeled by replacing one Fe (or C) atom in the unit cell with the alloying element. We considered the alloying atom substituting the Fe atom on all possible Fe-occupied Wyckoff sites. Al, Si, P, and S were also considered on the C site of all the carbides. Alloying-element-substituted iron (ferrite solid solution) was modeled with $Fe_{127}M$. Similarly, alloying-element-substituted Fe_3C, Fe_5C_2, and η-Fe_2C were modeled with $Fe_{11}MC_4$ (or $Fe_{12}C_3M$ or for the $2 \times 2 \times 2$ supercell as $Fe_{95}MC_4$ or $Fe_{96}C_{31}M$), $Fe_{19}MC_8$ (or $Fe_{20}C_7M$), and $Fe_{47}MC_{24}$ (or $Fe_{48}C_{23}M$), respectively.

III. RESULTS AND DISCUSSION

A. *Crystal Structure and Formation Enthalpy of Pure Carbides*

Fe_3C[47] and η-Fe_2C[4,48–50] crystallize in an orthorhombic unit cell with 16 and 6 atoms, respectively, whereas Fe_5C_2[51–55] crystallizes in a monoclinic unit cell with 28 atoms. The first-principles structurally optimized crystal structure parameters along with the experimental results are given in Table I. The crystal structures of the carbides with the fractional coordinates of the atoms on various Wyckoff sites agree well with experiments and previous first-principles calculations. The formation enthalpies of pure Fe_3C, Fe_5C_2, and Fe_2C are 16 meV/atom, 13 meV/atom, and 5 meV/atom, respectively. Our results are in good agreement with previous first-principles results.[6,13,23,26–28,33,56,57] Formation enthalpies, which we consider too high for this class of carbides, of 1.6 eV/atom and 1.3 eV/atom for Fe_5C_2 and η-Fe_2C, respectively, have been reported.[7] A positive formation enthalpy implies that the compound is not stable compared with the elements in their standard states (Eq. [2]). Accordingly, the carbides in the order of decreasing stability are η-Fe_2C, Fe_5C_2, and Fe_3C, which is consistent with earlier calculations.[56,57] It is interesting to note that these carbides also occur in the same sequence during precipitation in steels.[6] Although the description of the properties of the pure carbides is of importance, here we are interested in the effect of alloying elements on the carbides.

Table I. Crystal Structures of Fe_3C, Fe_5C_2, and η-Fe_2C

Carbide (Sp. Gp. No., Pearson Sym.)	Lattice Parameters [Å]	Atom (Site)	Fractional Coordinates
Fe_3C	a = 5.032(5.090)	C(4c)	0.876(0.877), 0.250(0.250), 0.438(0.444)
(62, oP16)	b = 6.708(6.744)	Fe1(4c)	0.035(0.037), 0.250(0.250), 0.837(0.840)
	c = 4.477(4.525)	Fe2(8d)	0.176(0.182), 0.068(0.067), 0.332(0.337)
Fe_5C_2	a = 11.579(11.563)	C(8f)	0.113(0.106), 0.186(0.189), 0.579(0.577)
(15, mC28)	b = 4.495(4.573)	Fe1(8f)	0.401(0.404), 0.084(0.095), 0.082(0.079)
	c = 4.975(5.058)	Fe2(8f)	0.214(0.213), 0.082(0.073), 0.310(0.314)
	β = 97.6(97.7)	Fe3(4e)	0.000(0.000), 0.067(0.073), 0.250(0.250)
η-Fe_2C	a = 4.708	C(2a)	0.000(0.000), 0.500(0.500), 0.000(0.000)
(58, oP6)	b = 4.281	Fe(4g)	0.346(0.333), 0.751(0.750), 0.000(0.000)
	c = 2.824		

The column labeled "Site" indicates both the multiplicity and the Wyckoff symbol. The numbers in parenthesis are experimental results obtained from Refs. 47, 54, and 4 for Fe_3C, Fe_5C_2, and η-Fe_2C, respectively.

B. *Supercell Size Effects*

To investigate the effect of increasing supercell size on partitioning enthalpies and other properties, we use supercells of different sizes for both bcc-Fe and cementite. In the case of bcc-Fe, we use $3 \times 3 \times 3$ and $4 \times 4 \times 4$ supercells, whereas for cementite, we use $1 \times 1 \times 1$ and $2 \times 2 \times 2$ supercells. In computing the partitioning enthalpies, the use of either a $3 \times 3 \times 3$ or a $4 \times 4 \times 4$ supercell of bcc-Fe does not change the partitioning enthalpies except for a few meV in the worst cases, indicating that the relaxation effects in a larger the smaller bcc-Fe supercell. When a larger $2 \times 2 \times 2$ cementite supercell is used instead of a $1 \times 1 \times 1$ supercell, the partitioning enthalpies changed significantly (Figure 1). Although the formation enthalpy and the crystal structure of pure cementite do not show any perceivable changes, the increase in supercell size leads to considerable changes in the partitioning enthalpies of the impurity-substituted carbides. This change is clearly noticeable in the case of the alloying elements that lead to large changes in volume of the alloying element substituted supercells, namely P, S, Nb, Mo, and W, along with Al and Si when substituted on the C site (Figure 2). The supercell effect is less pronounced in the case of Ti, V, Cr, Mn, Co, Ni, and Cu where the volume change is much less compared with the former group of elements. The increase in carbide supercell size, thus, generally leads to a less stable carbide and, hence, a stronger preference of the bcc-Fe phase. This is easily rationalized: In the small supercell, oversized atoms are accommodated mostly by expanding the volume, whereas in larger supercells, the distortion of the carbide lattice predominates. The expansion of the small supercell does not take into account that this volume expansion will lead to elastic strains at larger lengths scales, and therefore, small supercell calculations energetically might be biased toward the carbide phase unless the actual alloying element concentrations in the carbide are representative for the supercell compositions. In the subsequent discussion, we refer to the results calculated using the larger $4 \times 4 \times 4$ and the $2 \times 2 \times 2$ bcc-Fe and cementite supercells.

C. *Site Preference of Alloying Elements in the Carbides*

Site preferences can be deduced either from formation enthalpies (Figure 3 and Table II) or partitioning enthalpies (Figure 4 and Table III). In Fe_3C, when substitution of the alloying elements is considered only on the metal site, all alloying elements prefer to occupy the 8d site.[20,31] When P and S are substituted on the metal sites, it is observed that there is a major reorganization of the nearest neighbor atoms. Fe atoms are observed to move closer to the P and S atoms, both of which have *p* valence electrons. No such reorganization was observed when the transition alloying elements with only *d* valence electrons occupied the Fe site. These

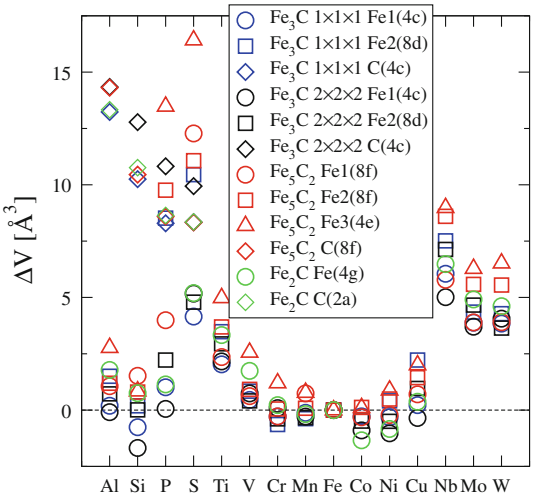

Fig. 2—Changes in volume of alloying element substituted carbide supercells with respect to the pure carbide supercell.

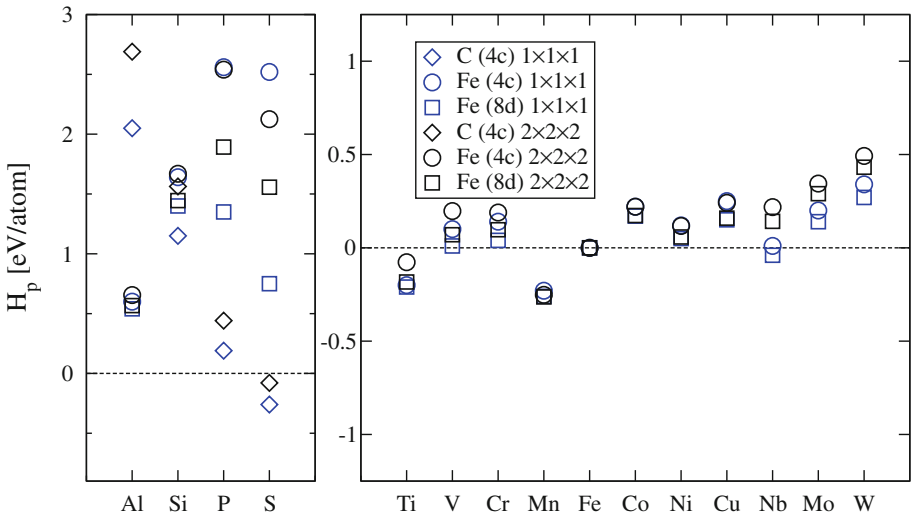

Fig. 1—Plot illustrating the supercell size effects for cementite. Enthalpies of preference using the $4 \times 4 \times 4$ bcc-Fe supercell along with $1 \times 1 \times 1$ and $2 \times 2 \times 2$ cementite supercells are shown.

observations, along with the fact that the C site has the maximum number of Fe neighbors in the carbide structures, prompted us to consider P and S along with Al and Si on the C site. As might be expected, P and S, on the basis of the strong bonding with the Fe atoms, preferred the C site over the Fe sites (Figure 4 and Table III). The case of Si is somewhat ambiguous: In the $1 \times 1 \times 1$ cementite supercell, there is a clear preference for the C site, whereas in the larger $2 \times 2 \times 2$ supercell, the Fe2(8d) and C sites are almost degenerate (Figure 1). It should be remarked, however, that Si strongly favors dissolution in the ferrite phase rather than in cementite. Al is most stable on the Fe2(8d) site. The preference of Al, Si for the Fe site and P, S for the C site from our $2 \times 2 \times 2$ supercell calculations agree well with previous results,[22] which were carried out at a lower kinetic energy cutoff (350 eV).

In Fe_5C_2, alloying elements prefer various sites (Figure 4 and Table III). The symmetry of the crystal structure is completely lost only on substitution of the alloying element on the Fe1(8f) or the Fe2(8f) sites. This loss in symmetry leads the atoms constituting the structure to have more degrees of freedom to relax, and hence, most of the alloying elements prefer to occupy either the Fe1(8f) or the Fe2(8f) site. All carbide formers like Ti, V, Nb, and Mo seem to prefer the Fe1(8f) site, which has four close C neighbors, two at approximately 2 Å, third at 2.4 Å, and a fourth at 2.8 Å. Although Al and Cu are not considered good carbide formers, they also prefer to occupy this site. Co occupies the Fe2(8f) site with the least number of C neighbors, two at approximately 2 Å and the third at approximately 2.4 Å. Ni and W do not show any preference between the Fe1(8f) or the Fe2(8f) sites. The Fe3(4e) site is preferred by Cr and Mn only. Cr and Mn have a stronger affinity for carbon than Fe and tend to be soluble in most carbide phases. The somewhat unique site preference of Cr and Mn may be caused by the rather small atomic size difference with Fe, which makes relaxation effects less important. Simultaneously, the Fe3 site provides 4 close C nearest neighbors at approximately 2 Å. Si, P, and S prefer to occupy the C site.

In Fe_2C, P, and S prefer to occupy the C site, whereas Al prefers the Fe site. Although Si prefers the C site in Fe_3C and Fe_5C_2, it prefers the Fe site Fe_2C.

D. *Volume Changes*

When fully relaxing the impurity substituted supercell, we make the implicit assumption that the supercell under investigation experiences no external stress. Although this assumption is valid for massive bulk materials, the assumption must be considered carefully when dealing with precipitate phases such as the ones being considered in this article. The precipitates are embedded in a ferrite matrix with which at least partial coherency exists, which leads to a strained impurity substituted precipitate phase. Changes in volume of the precipitate phase can increase or decrease the strain. In light of this, it is worthwhile to examine the volume changes brought about by the substitution of the alloying elements on various sites. Situations can be envisaged where although it might be energetically favorable to occupy a certain site, the strain effects might not actually allow such preference. Such a situation seems to manifest clearly in the case of Si. Although the preference in energy between the Fe sites and the C site is little, the volume change brought about by its substitution on the C site is much higher than its substitution on the Fe sites (10 to 15 $Å^3$ *vs* −2.5 to 2.5 $Å^3$) (see Figure 2). It is harder to make such an argument in the case of P and S because although the volume changes on the C site are higher compared with the changes on the Fe site, the preference to the C site is much larger compared with Si.

E. *Stabilization of Carbides with Respect to Ferrite*

In our previous work,[31] we showed how using ΔH_f to determine stabilization of cementite gives results that do not agree with experiments in the case of Al, Mo, and W. The case of Al is striking as it is predicted to stabilize cementite almost twice as much as Mn. Al, of course, does not stabilize cementite, whereas Mn is experimentally known to partition to, and hence stabilize, cementite[58–60] (for more references, Reference 31). Despite using a $4 \times 4 \times 4$ bcc-Fe and a $2 \times 2 \times 2$ cementite supercell in the current work instead of the $3 \times 3 \times 3$ and $1 \times 1 \times 1$ supercells, respectively, as used in Reference 31, our conclusions about the partitioning and stabilization of the alloying elements between cementite and ferrite remain qualitatively the same when considering partitioning on the Fe site. Please note that we list H_f in Table III of Ref. 31, while in Table II of this article, we list ΔH_f.

In the case of Fe_5C_2, examining ΔH_f might suggest that Al, Ti, V, Cr, Mn, and Nb stabilize the carbide phase, whereas the rest of the alloying elements destabilize it (Table II and Figure 3). As in the case of cementite, this is a misinterpretation of the data.

However, when we consider the reference states of the alloying elements correctly *via* the partitioning enthalpies instead of formation enthalpies, both Al[61,62] and Si[59,60,63–65] destabilize the formation of not only cementite but also all the carbide phases (Figure 4 and Table III) regardless of whether Fe or C site substitution is considered. This finding shows that the conclusions about stabilization of carbides with respect to ferrite based on partitioning enthalpies are more reliable than the ones based on formation enthalpies. Not only do both Al and Si destabilize all three carbide phases, but also Si destabilizes them more than Al (Figure 4).

P, Co, Ni, Cu, Mo, and W also destabilize the three carbides considered in this article, although not nearly as strongly as Si and Al. Surprisingly, S on the C site stabilizes Fe_3C and Fe_5C_2 while destabilizing Fe_2C. Ti and Mn stabilize the three carbide phases while Nb stabilizes cementite and Hägg carbides but not η-Fe_2C. V and Cr destabilize Fe_3C and Fe_5C_2 by a negligible amount while V destabilizes η-Fe_2C.

However, the *ab initio* computed partitioning enthalpies do not agree with all experimental observations. Cr is known to partition, and hence stabilize, Fe_3C.[59,60,63]

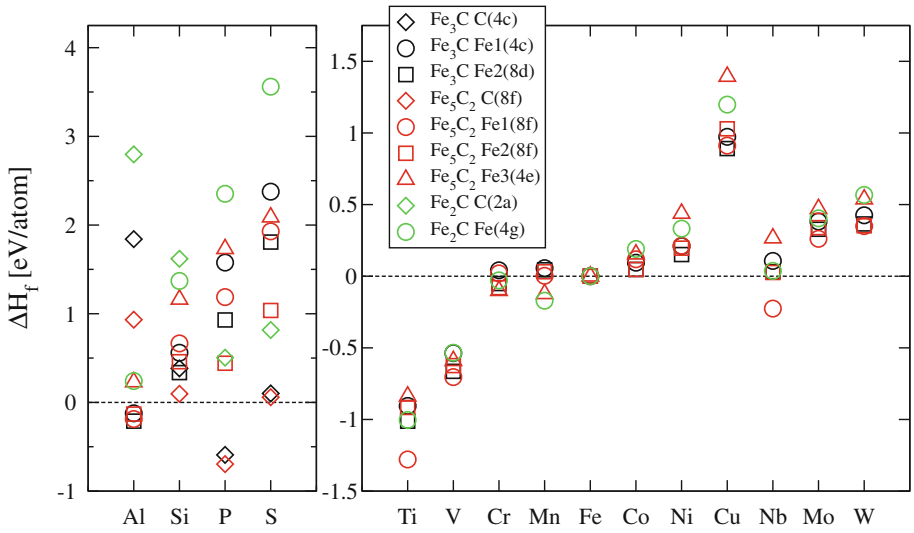

Fig. 3—Formation enthalpies of alloying element substituted carbides as defined in Eq. [3].

Table II. Formation Enthalpies of Alloying-Element-Substituted Carbides with Respect to the Pure Carbide, ΔH_f (eV/atom)

	Fe_3C			Fe_5C_2				Fe_2C	
Element	Fe1(4c)	Fe2(8d)	C(4c)	Fe1(8f)	Fe2(8f)	Fe3(4e)	C(8f)	Fe(4g)	C(2a)
Al	−0.12	−0.21	1.84	−0.18	−0.13	0.23	0.93	0.24	2.80
Si	0.56	0.34	0.38	0.67	0.46	1.16	0.10	1.37	1.62
P	1.58	0.93	−0.59	1.19	0.44	1.73	−0.69	2.35	0.50
S	2.38	1.81	0.10	1.93	1.04	2.09	0.06	3.56	0.82
Ti	−0.91	−1.01	–	−1.28	−0.91	−0.84	–	−1.00	–
V	−0.54	−0.66	–	−0.70	−0.62	−0.59	–	−0.54	–
Cr	0.04	−0.05	–	0.02	−0.08	−0.10	–	−0.03	–
Mn	0.06	0.05	–	0.01	0.03	−0.12	–	−0.17	–
Fe	0.00	0.00	–	0.00	0.00	0.00	–	0.00	–
Co	0.09	0.05	–	0.12	0.05	0.16	–	0.19	–
Ni	0.21	0.15	–	0.21	0.20	0.44	–	0.33	–
Cu	0.97	0.89	–	0.91	1.03	1.40	–	1.20	–
Nb	0.11	0.03	–	−0.22	0.03	0.27	–	0.04	–
Mo	0.38	0.33	–	0.26	0.34	0.47	–	0.40	–
W	0.43	0.37	–	0.35	0.35	0.54	–	0.57	–

The alloying element has been considered on all possible Fe Wyckoff sites of the carbide. Formation enthalpies are calculated as defined in Eq. [3] with $k = 32, 4, 24$ for Fe_3C, Fe_5C_2, and η-Fe_2C, respectively, and with $p = 128$ for bcc-Fe.

In fact, more so than Mn. Alas, Cr is computed to destabilize slightly and hence partition away from cementite, contrary to experimental evidence.[59,60,63] Possibly, Cr-rich carbides form prior to Fe-based carbides and act as nucleation sites for the cementite and other Fe-based carbides. If those initial Cr-rich carbides are small enough they might not be recognized as distinct phases. We do compute that Mn stabilizes Fe_3C in agreement with experimental observations.[58–60,63] Mn is computed to stabilize Fe_5C_2 and Fe_2C even a little more. Our computed partitioning enthalpies do not reflect correctly the fact that Mo[59,60,63] and W[63] also partition to cementite, although the enthalpies involved are rather small. It should be noted that all our calculations are based on enthalpies obtained at 0 K. The neglect of entropy (S) changes at finite temperature is less likely to be tenable when enthalpy changes are of order TS, where S could be mainly the result of alloy element-induced magnetic (dis)ordering, which could be of order k_B. Given that experimental measurements are typically in the neighborhood of the ferrite-austenite transition temperature, it follows that partitioning enthalpies less than 0.1 eV are rather inconclusive.

F. *Relative Stabilization of Carbides*

Si, P, S, and Al destabilize η-Fe_2C much more than cementite and Hägg carbide. All alloying elements except Mn destabilize η-Fe_2C relative to Fe_3C and Fe_5C_2. At this juncture, it is interesting to note that Mn also stabilizes ϵ-Fe_2C, a carbide closely related to η-Fe_2C, over cementite.[27] The competition between cementite and Hägg carbide is not nearly as strongly affected by alloying additions as the competitions

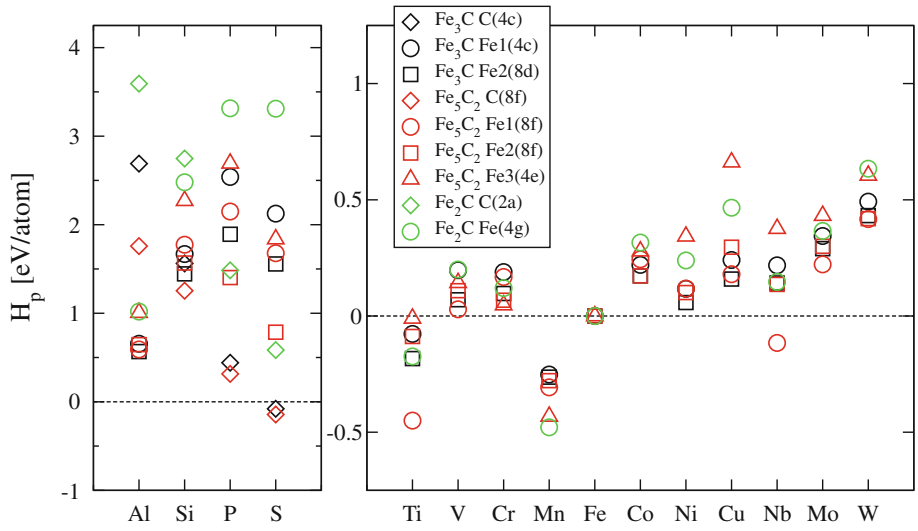

Fig. 4—Partitioning enthalpies of alloying element substituted carbides as defined in Eqs. [6] and [8].

Table III. Partitioning Enthalpies of Alloying-Element-Substituted Carbides, $H_p^{(Fe)}$ (eV/atom)

	Fe_3C			Fe_5C_2				Fe_2C	
Element	Fe1(4c)	Fe2(8d)	C(4c)	Fe1(8f)	Fe2(8f)	Fe3(4e)	C(8f)	Fe(4g)	C(2a)
Al	0.66	0.57	2.69	0.59	0.65	1.01	1.76	1.02	3.59
Si	1.67	1.45	1.56	1.77	1.57	2.27	1.25	2.48	2.75
P	2.54	1.89	0.44	2.15	1.40	2.69	0.31	3.31	1.49
S	2.13	1.56	−0.08	1.68	0.79	1.84	−0.14	3.31	0.58
Ti	−0.08	−0.18	–	−0.45	−0.09	−0.01	–	−0.17	–
V	0.20	0.07	–	0.03	0.11	0.14	–	0.20	–
Cr	0.19	0.10	–	0.17	0.07	0.05	–	0.12	–
Mn	−0.25	−0.26	–	−0.31	−0.28	−0.43	–	−0.48	–
Fe	0.00	0.00	–	0.00	0.00	0.00	–	0.00	–
Co	0.22	0.17	–	0.24	0.17	0.28	–	0.32	–
Ni	0.12	0.06	–	0.12	0.10	0.34	–	0.24	–
Cu	0.24	0.16	–	0.18	0.30	0.66	–	0.47	–
Nb	0.22	0.14	–	−0.12	0.14	0.38	–	0.15	–
Mo	0.34	0.29	–	0.22	0.30	0.43	–	0.37	–
W	0.49	0.43	–	0.42	0.42	0.61	–	0.63	–

The alloying element has been considered on all possible Fe Wyckoff sites of the carbide. Partitioning enthalpies are calculated as defined in Eqs. [6] and [8] with k = 32, 4, 24 for Fe_3C, Fe_5C_2, and η-Fe_2C, respectively, and with p = 128 for bcc-Fe.

involving η-Fe_2C. Si, Mo, and W are found to disfavor cementite less than Hägg carbide, whereas Ti, Mn, and Nb promote Hägg carbide at the expense of cementite. This is in line with the complete intermixing between Fe_5C_2 and Mn_5C_2,[58] whereas such thermodynamically favorable dissolution does not exist for cementite.[26] Our results indicate that Mn stabilizes η-Fe_2C and Fe_5C_2 approximately equally.

IV. CONCLUSIONS

First-principles calculations on the alloying element substituted carbides Fe_3C, Fe_5C_2, and η-Fe_2C show that Si and Al destabilize the formation of carbides, and Si is the most effective. P and S prefer to occupy the C site in all the carbides, whereas Si weakly prefers to occupy the C site in two of them, Fe_3C and Fe_5C_2. On a per-atomic-fraction basis, Si is approximately twice as effective as Al for carbide suppression. All alloying elements considered, except Mn, destabilize η-Fe_2C relative to Fe_3C and Fe_5C_2. The competition between Fe_3C and Fe_5C_2 is not so strongly affected by alloying elements. Si, Mo, and W disfavor Fe_5C_2 more than Fe_3C, whereas Ti, Mn, and Nb stabilize Fe_5C_2 over Fe_3C. Mn stabilizes both Fe_5C_2 and η-Fe_2C to a comparable degree over Fe_3C. At a finite temperature the observed partitioning behaviors of Cr, V, Mo, and W are not explained satisfactorily based on first-principles zero-temperature partitioning enthalpies. It is to be borne in mind that experimental observations pertain to carbides in the paramagnetic state, whereas the first-principles calculations pertain to the ferromagnetic state at zero temperature. Although configurational entropy effects can be shown to play a minor role at the temperatures of interest in relation to the computed

enthalpy changes, the same cannot be said of magnetic entropies. Possibly, by considering the carbides in a disordered local moment state and by explicitly considering magnetic entropy contributions to the free energy, a better agreement with experiment might be found. Experimentally, there is a possibility for misinterpretations if Cr-, V-, Mo-, or W-rich carbides form prior to Fe-based carbides and then subsequently act as nucleation sites for cementite or other Fe-based carbides. If those initial alloy element-rich carbides are small enough, they might not be recognized as distinct phases.

ACKNOWLEDGEMENTS

This research was carried out under project number MC5.05239 in the framework of the Research Program of the Materials innovation institute M2i (www.m2i.nl). The authors gratefully acknowledge the cooperation with Tata Steel Nederland Technology BV and the fruitful discussions with Jeroen Colijn, Winfried Kranendonk, and Bernard Ennis.

OPEN ACCESS

REFERENCES

1. L.J.E. Hofer and E.M. Cohn: *Nature*, 1951, vol. 167, pp. 977–78.
2. J.W. Christian: *The Theory of Transformation in Metals and Alloys*, Pergamon Press, Amsterdam, The Netherlands, 2002.
3. M. Manes, A.D. Damick, M. Menster, E.M. Cohn, and L.J.E. Hofer: *J. Am. Chem. Soc*., 1952, vol. 74, pp. 6207–09.
4. Y. Hirotsu and S. Nagakura: *Acta Metall*., 1972, vol. 20, pp. 645–55.
5. M.J. van Genderen, A. Böttger, R.J. Cernik, and E.J. Mittemeijer: *Metall. Trans. A*, 1993, vol. 24A, pp. 1965–73.
6. C.M. Fang, M.H.F. Sluiter, M.A. van Huis, C.K. Ande, and H.W. Zandbergen: *Phys. Rev. Lett*., 2010, vol. 105, pp. 055503(1–4).
7. H.I. Faraoun, Y.D. Zhang, C. Esling, and H. Aourag: *J. Appl. Phys*., 2006, vol. 99, pp. 093508(1–8).
8. Y. Zhang, X. Zhao, N. Bozzolo, C. He, L. Zuo, and C. Esling: *ISIJ Int*., 2005, vol. 45, pp. 913–17.
9. A. Dick, F. Körmann, T. Hickel, and J. Neugebauer: *Phys. Rev. B*, 2011, vol. 84, pp. 125101(1–9).
10. W.C. Chiou and E.A. Carter: *Surf. Sci*., 2003, vol. 530, pp. 87–100.
11. I.R. Shein, N.I. Medvedeva, and A.L. Ivanovskiĭ: *Physica B*, 2006, vol. 371, pp. 126–32.
12. C. Jiang, B.P. Uberuaga, and S.G. Srinivasan: *Acta Mater*., 2008, vol. 56, pp. 3236–44.
13. B. Hallstedt, D. Djurovic, J. von Appen, R. Dronskowski A. Dick, F. Körmann, T. Hickel, and J. Neugebauer: *CALPHAD*, 2010, vol. 34, pp. 129–33.
14. C. Jiang, S.G. Srinivasan, A. Caro, and S. A. Maloy: *J. Appl. Phys*., 2008, vol. 103, pp. 043502(1–8).
15. Z.Q. Lv, S.H. Sun, P. Jiang, B.Z. Wang, and W.T. Fu: *Comput. Mater. Sci*., 2008, vol. 42, pp. 692–97.
16. M. Nikolussi, S.L. Shang, T. Gressmann, A. Leineweber, E.J. Mittemeijer, Y. Wang, and Z.-K. Liu: *Scripta. Mater*., 2008, vol. 59, pp. 814–17.
17. H. Ledbetter: *Mater. Sci. Eng. A*, 2010, vol. 527, pp. 2657–61.
18. N.I. Medvedeva, L.E. Kar'kina, and A.L. Ivanovskiĭ: *Phys. Solid State*, 2006, vol. 48, pp. 15–19.
19. N. Medvedeva, I. Shein, O. Gutina, and A. Ivanovskiĭ: *Phys. Solid State*, 2007, vol. 49, pp. 2298–302.
20. I.R. Shein, N.I. Medvedeva, and A.L. Ivanovskiĭ: *Phys. Status Solidi B*, 2007, vol. 244, pp. 1971–81.
21. N. Medvedeva, I. Shein, M. Konyaeva, and A. Ivanovskiĭ: *Phys. Met. Metall*., 2008, vol. 105, pp. 568–73.
22. O.Y. Gutina, N.I. Medvedeva, I.R. Shein, A.L. Ivanovskiĭ, and J.E. Medvedeva: *Phys. Status Solidi B*, 2009, vol. 246, pp. 2167–71.
23. J.H. Jang, I.G. Kim, and H.K.D.H. Bhadeshia: *Comput. Mater. Sci*., 2009, vol. 44, pp. 1319–26.
24. M. Konyaeva and N. Medvedeva: *Phys. Solid State*, 2009, vol. 51, pp. 2084–89.
25. X. Wang and M. Yan: *Int. J. Mod. Phys. B*, 2009, vol. 23, pp. 1135–40.
26. J. von Appen, B. Eck, and R. Dronskowski: *J. Comput. Chem*., 2010, vol. 31, pp. 2620–27.
27. J.H. Jang, I.G. Kim, and H.K.D.H. Bhadeshia: *Scripta. Mater*., 2010, vol. 63, pp. 121–23.
28. J.H. Jang, I.G. Kim, and H.K.D.H. Bhadeshia: *Mater. Sci. Forum*, 2010, vol. 638 (642), pp. 3319–24.
29. Z.Q. Lv, W.T. Fu, S.H. Sun, Z.H. Wang, W. Fan, and M.G. Qv: *Solid State Sci*., 2010, vol. 12, pp. 404–08.
30. Z.Q. Lv, W.T. Fu, S.H. Sun, X.H. Bai, Y. Gao, Z.H. Wang, and P. Jiang: *J. Magn. Magn. Mater*., 2011, vol. 323, pp. 915–19.
31. C.K. Ande and M.H.F. Sluiter: *Acta Mater*., 2010, vol. 58, pp. 6276–81.
32. C.T. Zhou, B. Xiao, J. Feng, J.D. Xing, X.J. Xie, Y.H. Chen, and R. Zhou: *Comput. Mater. Sci*., 2009, vol. 45, pp. 986–92.
33. K.O.E. Henriksson, N. Sandberg, and J. Wallenius: *Appl. Phys. Lett*., 2008, vol. 93, pp. 191912(1–3).
34. P.J. Steynberg, J.A. van den Berg, and W.J. van Rensburg: *J. Phys. Condens. Matter*., 2008, vol. 20, pp. 064238(1–11).
35. R. Benedek, A. van de Walle, S.S.A. Gerstl, M. Asta, D.N. Seidman, and C. Woodward: *Phys. Rev. B*, 2005, vol. 71, pp. 094201(1–12).
36. P. Hohenberg and W. Kohn: *Phys. Rev*., 1964, vol. 136, pp. B864–71.
37. W. Kohn and L.J. Sham: *Phys. Rev*., 1965, vol. 140, pp. A1133–38.
38. G. Kresse and J. Hafner: *Phys. Rev. B*, 1993, vol. 48, pp. 13115–18.
39. G. Kresse and J. Furthmüller: *Comput. Mater. Sci*., 1996, vol. 6, pp. 15–50.
40. G. Kresse and J. Furthmüller: *Phys. Rev. B*, 1996, vol. 54, pp. 11169–86.
41. P.E. Blöchl: *Phys. Rev. B*, 1994, vol. 50, pp. 17953–79.
42. J.P. Perdew, J.A. Chevary, S.H. Vosko, K.A. Jackson, M.R. Pederson, D.J. Singh, and C. Fiolhais: *Phys. Rev. B*, 1992, vol. 46, pp. 6671–87.
43. S.H. Vosko, L. Wilk, and M. Nusair: *Can. J. Phys*., 1980, vol. 58, pp. 1200–11.
44. P.E. Blöchl, O. Jepsen, and O.K. Andersen: *Phys. Rev. B*, 1994, vol. 49, pp. 16223–33.
45. H.J. Monkhorst and J.D. Pack: *Phys. Rev. B*, 1976, vol. 13, pp. 5188–92.
46. M.H.F. Sluiter: *Mat. Res. Soc. Proc*., in D. Seidman, P. Bellon, C. Abromeit, and J.-L. Boquet, eds., 2006 pp. 43–48.
47. E.J. Fasiska and G.A. Jeffrey: *Acta Crystallogr*., 1965, vol. 19, pp. 463–71.
48. K.H. Jack: *J. Iron Steel Inst*., 1951, vol. 169, pp. 26–36.
49. K.H. Jack: *Acta Crystallogr*., 1952, vol. 5, pp. 404–11.
50. S. Nagakura and S. Oketani: *Trans. ISIJ*, 1968, vol. 8, pp. 265–94.
51. G. Hägg: *Z. Phys. Chem. B*, 1931, vol. 12, pp. 33–56.
52. J.P. Senateur, D. Fruchart, and A. Michel: *Comptes Rendus Acad. Sci*., 1962, vol. 255, pp. 1615–16.
53. K.H. Jack and S.A. Wild: *Acta Crystallogr*., 1966, vol. S21, p. A81.
54. J.P. Senateur: *Ann. de Chimie*, 1967, vol. 2, pp. 103–22.
55. J.J. Retief: *Powder Diffract*., 1999, vol. 14, pp. 130–32.
56. M. Widom and M. Mihalkovic: *J. Mater. Res*., 2005, vol. 20, pp. 237–42.
57. C.M. Fang, M.A. van Huis, and H.W. Zandbergen: *Scripta Mater*., 2010, vol. 63, pp. 418–21.
58. G.P. Huffman, P.R. Errington, and R.M. Fisher: *Phys. Status Solidi B*, 1967, vol. 22, pp. 473–81.
59. R.C. Thomson and M.K. Miller: *Appl. Surf. Sci*., 1995, vols. 87–88, pp. 185–93.

60. R.C. Thomson and M.K. Miller: *Acta Mater.*, 1998, vol. 46, pp. 2203–13.
61. W.C. Leslie and G.C. Rauch: *Metall. Trans. A*, 1978, vol. 9A, pp. 343–49.
62. L. Qingdong, L. Wenqing, W. Zemin, and Z. Bangxin: *Acta Metall. Sinica*, 2009, vol. 45, pp. 1281–87.
63. M. Ko, T. Sakuma, and T. Nishizawa: *J. Jpn. Inst. Met.*, 1976, vol. 40, pp. 593–601.
64. E. Kozeschnik and H.K.D.H. Bhadeshia: *Met. Mat. Sci. Tech*, 2008, vol. 24, pp. 343–47.
65. Q. Liu, Y. Chu, Z. Wang, W. Liu, and B. Zhou: *Acta Metall. Sinica*, 2008, vol. 44, pp. 1281–85.